Arch. Mech., 40, 2–3, pp. 183–199, Warszawa 1988

Free vibrations of thin, elastic, segmented shells of revolution reinforced with circumferential rings

B. BŁOCKA (GDAŃSK)

THE SUBJECT-MATTER of this paper is a method for calculation of frequencies and modes of free vibration of thin, elastic, segmented shells of revolution reinforced with internal or external circumferential rings. The shape of the meridian and the change of thickness of the shell in the meridional direction may be arbitrary. Material and structural orthotropy of the shell have also been taken into account. The problem is posed in a variational form. The functional associated with Hamilton's principle has been expanded into trigonometric series in the circumferential direction and finite-difference method has been applied along the meridian. In consequence, the problem has been converted into a generalized eigen-value problem. Numerical examples, calculated with the program DYSAR based on an algorithm presented here, expose the possibilities of the method and the program itself. Analysis and comparison of these numerical results with the experimental data published in the literature confirm their correctness and accuracy, which turn out to be quite sufficient for practical applications even in the case of relatively small number of nodes of the finite difference net.

W pracy podano metodę obliczania częstości i postaci drgań własnych cienkich, sprężystych, segmentowych powłok obrotowych, wzmocnionych wewnętrznymi lub zewnętrznymi pierścieniami kołowymi. Opracowany algorytm uwzględnia dowolną geometrię południka powłoki, zmianę jej grubości wzdłuż południka, ortotropię materiału oraz ortotropię konstrukcyjną. Zadanie sformułowano w postaci wariacyjnej. Zbudowany funkcjonał typu Hamiltona dla drgań harmonicznych rozwinięto w szeregi trygonometryczne w kierunku obwodowym oraz zdyskretyzowano w kierunku południkowym stosując różnice skończone. W rezultacie zadanie sprowadzono do uogólnionego problemu na wartości własne. Przykłady numeryczne, obliczone programem DYSAR opracowanym na podstawie przedstawionego algorytmu, pokazują efektywność metody i programu. Analiza i porównanie wyników obliczeń z danymi eksperymentalnymi zamieszczonymi w literaturze wskazują na ich poprawność i dokładność wystarczającą dla celów praktycznych, nawet przy stosunkowo niewielkiej liczbie węzłów siatki różnicowej.

В работе приведен метод расчета частоты и формы собственных колебаний тонких упругих сегментных оболочек вращения, упрочненных внутренними или внешними круговыми кольцами. Разработанный алгоритм учитывает произвольную геометрию меридиана оболочки, изменение ее толщины вдоль меридиана, ортотропию материала и конструкционную ортотропию. Задача поставлена вариационном виде. Постоенный функционал типа Гамильтона для гармонических колебаний разложен в тригонометрические ряды по контуру и дискретизирован по контуру в направлении меридиана с использованием конечной разности. В результате задача сводится к обобщенной задаче на собственные значения. Числовые примеры, расчитанные по программе DYSAR, разработанной на основе представленного алгоритма, иллюстрируют эффективность метода и программы. Анализ и сравнение результатов расчетов с экспериментальными данными, находящимися в литературе подтверждают их правильность и точность, достаточную для практических целей, даже при относительно небольшом количестве узлов разностной сетки.

1. Introduction

A NUMBER of papers have been devoted to the problem of free vibration analysis of thin elastic shells of revolution reinforced with circular rings. At first mainly analytical methods

were applied, restricted mostly to special shell geometries or to special simplified theories with simple boundary conditions [10]. A series of special methods of analysis and computer programs for dynamical calculations of shells of revolution of arbitrary meridional geometry were created with the application of computer techniques. Among the methods applied were: finite element method [16, 19], the numerical integration method [6, 11, 17], the classical finite-difference method [1], or the energy finite-difference method [4]. Utilization of large computer system like SAP IV, ASKA based on the finite element method is also possible; however, it is not convenient due to the complicated process of input data preparations and long computer time, when compared with the specialized methods.

This paper presents a modified method of free vibration analysis of a thin-walled structure, modelled by a thin elastic segmented shell of revolution. Within this model the geometry of the meridian of a shell segment may be arbitrary, and so may be the change of the shell thickness along the meridian. The orthotropy of the shell material and the structural orthotropy arising from the presence of the circular reinforcing rings, are also taken into account. Arbitrary homogeneous displacement conditions may be imposed on the boundaries and the joints between the neighbouring segments.

The problem has been formulated in the variational form and then solved by separation of variables. The independent variables of the functional (the displacements of the middle surface of the shell) are expanded into trigonometric series in the circumferential direction. Then they are discretized in the meridional direction. Imposition of the stationarity condition on the resulting algebraic quadratic form yields a generalized eigenvalue problem, numerical analysis of which leads to the free-vibration frequencies and modes.

A similar method was applied by BUSHNELL [4]. In contradistinction to the papers by Bushnell, the Lagrange multiplier method has not been applied here to the boundary conditions and the conditions of compatibility of the displacements between the shell segments. Appropriate elimination of rows and columns and aggregation of the stiffness and mass matrices have been applied, instead, in a way similar to the one employed in the finite element method [9]. This modification eliminates fictitious nodes, apearing beyond the boundary region of the shell and arising from the finite difference scheme assumed. Otherwise, these fictitious nodes might generate additional non-existing eigenvalues. Besides, this procedure decreases the dimension of the eigen-value problem. This is particularly important when the system comprises many segments or is reinforced along the meridians, since the harmonics are coupled in the latter case [3].

The numerical examples presented in the paper show correctness and efficiency of this modified method and broad capabilities of application of the program DYSAR.

2. Basic assumptions

It is assumed that the shell as well as the beam elements are thin. This allows to express all the quantities describing the state of displacement of the shell through the displacements of its middle surface, and the state of displacement of the stiffeners through the displacements of the centroids of their cross-sections. The analysis is based on the Sanders' variant

of the linear shell theory [15] and the theory of weakly curved rods [14]. Besides, it is assumed that the rings are fastened to the shell along the parallels and the joint of the middle surface with the centroids of their cross-sections can be modelled by stiff elements.

Figure 1 presents the local (s, θ, ζ) and the global (x, θ, z) systems of coordinates on the shell and the main geometric parameters R_1, R_2, r describing the middle surface of a shell of revolution. Figure 2, instead, illustrates the parameters describing location of

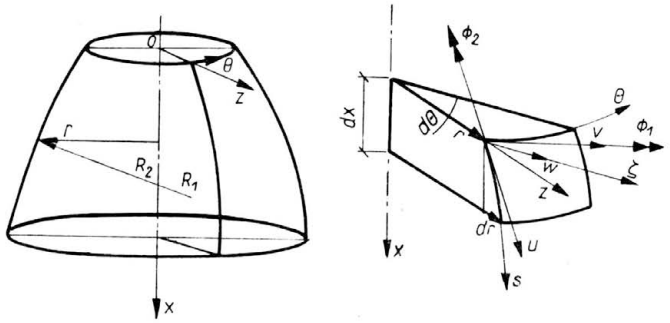

FIG. 1. Geometry of a shell of revolution; local (s, θ, ζ) and global (x, θ, z) systems of coordinates.

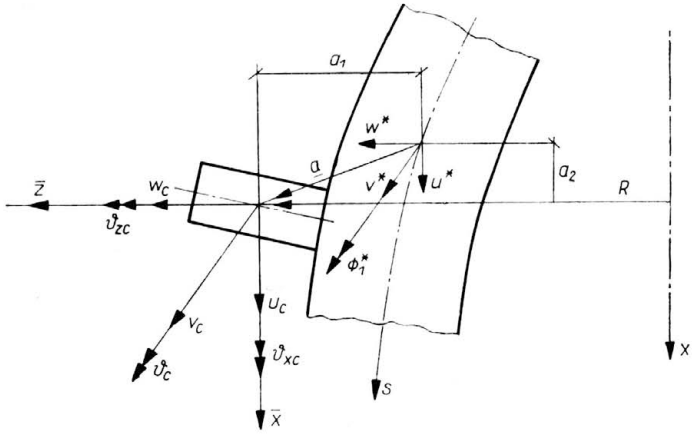

FIG. 2. Location of a circular ring; displacements and rotations of the cross-section of the ring u_c, v_c, w_c, ϑ_c, ϑ_{xc}, ϑ_{zc}; displacements of the shell in the global system u^*, v^*, w^* ϕ_1^*.

the ring stiffener on the shell. It is determined by a vector $\mathbf{a}(a_2, 0, a_1)$ lying in the plane perpendicular to the middle surface and the meridional coordinate s_j along the line of joints between the ring and the shell. External and internal circular rings may be stiffeners as well as boundary elements or elements joining two neighbouring shell segments.

3. Vartiational formulation

The problem of free vibrations of thin elastic segmented shells of revolution reinforced by circular rings has been formulated as the problem of minimization of the functional associated with Hamilton's principle, namely

$$\delta H = \delta \int_{t_0}^{t_1} (T-E)dt = 0, \tag{3.1}$$

where, in the case of free vibrations, E denotes the elastic and T the kinetic energies of the system. Particular component parts of these energies may be presented in the form

$$E_s = \frac{1}{2}\int_s \int_\theta \mathbf{n}_s^T \boldsymbol{\epsilon}_s r\,d\theta\,ds, \qquad E_c = \frac{1}{2}\int_\theta \mathbf{n}_c^T \boldsymbol{\epsilon}_c R\,d\theta,$$
$$T_s = \frac{\omega^2}{2}\int_s \int_\theta \mathbf{u}_s \overline{\mathbf{M}}_s \mathbf{u}_s r\,d\theta\,ds, \qquad T_c = \frac{\omega^2}{2}\int_\theta \mathbf{u}_c^T \overline{\mathbf{M}}_c \mathbf{u}_c R\,d\theta. \tag{3.2}$$

Here $\mathbf{n}_s$ and $\mathbf{n}_c$ are generalized vectors of forces in the shell and the ring, respectively, and their components are as follows:

$$\mathbf{n}_s = \{N_{11}N_{22}2\overline{N}_{12}M_{11}M_{22}2\overline{M}_{12}\}^T, \qquad \mathbf{n}_c = \{N_c M_{zc} M_{xc} M_c\}^T,$$
$$\overline{N}_{12} = \frac{1}{2}(N_{12}+N_{21}), \qquad \overline{M}_{12} = \frac{1}{2}(M_{12}+M_{21}). \tag{3.3}$$

The quantities $\boldsymbol{\epsilon}_s$, $\boldsymbol{\epsilon}_c$ with the components

$$\boldsymbol{\epsilon}_s = \{\varepsilon_{11}\varepsilon_{22}\varepsilon_{12}\varkappa_{11}\varkappa_{22}\overline{\varkappa}_{12}\}^T, \qquad \overline{\varkappa}_{12} = \frac{1}{2}(\varkappa_{12}+\varkappa_{21}),$$
$$\boldsymbol{\epsilon}_c = \{\varepsilon_c \varkappa_{xc} \varkappa_{zc} \varkappa_c\}^T, \tag{3.4}$$

are the corresponding vectors of strain in the shell and the ring, respectively. $\mathbf{M}_s$, $\mathbf{M}_c$ are the corresponding matrices of inertia coefficients, and $\mathbf{u}_s$, $\mathbf{u}_c$ vectors of generalized displacements in the shell and the ring. Their components are the displacements and rotations

$$\mathbf{u}_s = \{u\,v\,w\phi_1\phi_2\}^T, \qquad \mathbf{u}_c = \{u_c v_c w_c \vartheta_{xc}\vartheta_{zc}\}^T. \tag{3.5}$$

Obviously, not all of these components are independent variables. The Kirchhoff–Love hypothesis yields the relations

$$\{\phi_1\phi_2\}^T = \mathsf{B}_s\mathbf{u}, \qquad \mathbf{u} = \{u\,v\,w\}^T, \tag{3.6}$$

$$\{\vartheta_{xc}\vartheta_{zc}\} = \mathsf{B}_c\mathbf{u}_c, \qquad \mathbf{u}_c = \{u_c v_c w_c \vartheta_c\}^T, \tag{3.7}$$

where B_s, B_c are differential operators describing the relations between the dependent and independent components of the vectors (3.5).

The variational formulation given here guarantees automatical fulfilment of the dynamical boundary conditions. So, the objective now is to find the stationary values of the functional H from (3.1) at some kinematical boundary conditions.

4. The boundary conditions

Homogeneous kinematical boundary conditions for the shell may be written down in the local coordinate system (s, θ, ζ) in the form

$$\{u_A v_A w_A \phi_A\}^T = \mathsf{G}\mathbf{u}|_{s=s_A}, \qquad \{u_B v_B w_B \phi_B\}^T = \mathsf{G}\mathbf{u}|_{s=s_B}, \tag{4.1}$$

where u_A, v_A, w_A, ϕ_A and u_B, v_B, w_B, ϕ_B denote generalized displacements of the shell middle surface on its boundaries, that is for $s = s_A$ and $s = s_B$, respectively. In the global coordinate system x, θ, z these conditions will assume the following form:

$$\{u_A^* v_A^* w_A^* \phi_A^*\}^T = \mathbf{G}^* \mathbf{u}|_{s=s_A}, \qquad \{u_B^* v_B^* w_B^* \phi_B^*\} = \mathbf{G}^* \mathbf{u}|_{s=s_B}. \tag{4.2}$$

Displacements u^*, v^*, w^*, ϕ_1^* in the global coordinate system are illustrated in the Fig. 2. The operators G and G*, appearing in the formulae (4.1) and (4.2), have the following representations:

$$\mathbf{G} = \begin{bmatrix} 1 & 0 & 0 \\ 0 & 1 & 0 \\ 0 & 0 & 1 \\ \dfrac{1}{R_1} & 0 & -\dfrac{\partial}{\partial_s} \end{bmatrix}, \qquad \mathbf{G}^* = \begin{bmatrix} \dfrac{r}{R_2} & 0 & -\dfrac{dr}{ds} \\ 0 & 1 & 0 \\ \dfrac{dr}{ds} & 0 & \dfrac{r}{R_2} \\ \dfrac{1}{R_1} & 0 & -\dfrac{\partial}{\partial s} \end{bmatrix}. \tag{4.3}$$

The boundary conditions (4.2) in the global coordinate system x, θ, z are also employed as the compatibility conditions between neighbouring segments of the shell system.

5. The constitutive and kinematical relations

The form of the constitutive and kinematical relations for the elements of the reinforced system of shells of revolution results from the hypothesis assumed for the model of the shell segments and circular rings. For the Sander's variant of the linear theory of shells [15] and the theory of weakly curved beams [14], the constitutive relations can be written in the form

$$\mathbf{n}_s = \mathbf{C}_s \boldsymbol{\epsilon}_s, \qquad \mathbf{n}_c = \mathbf{C}_c \boldsymbol{\epsilon}_c, \tag{5.1}$$

where $\mathbf{C}_s$ and $\mathbf{C}_c$ are elasticity matrices of the shell and the ring, respectively [2].

The relations between the strains and displacements in the shell and ring may be formulated as a function of independent displacement parameters

$$\boldsymbol{\epsilon}_s = \mathbf{A}_s \mathbf{u}, \qquad \boldsymbol{\epsilon}_c = \bar{\mathbf{A}}_c \bar{\mathbf{u}}_c, \tag{5.2}$$

and the differential operators $\mathbf{A}_s$ and $\mathbf{A}_c$ are given explicitly in [2].

Employing (5.1) and (5.2), the elastic energies of the shell segment and the ring may now be presented as functions of the displacement vectors $\mathbf{u}$, $\bar{\mathbf{u}}_c$.

$$E_s = \frac{1}{2} \int_s \int_\theta (\mathbf{A}_s \mathbf{u})^T \mathbf{C}_s \mathbf{A}_s \mathbf{u} r \, d\theta \, ds, \qquad E_c = \frac{1}{2} (\bar{\mathbf{A}}_c \bar{\mathbf{u}}_c)^T \mathbf{C}_c \bar{\mathbf{A}}_c \bar{\mathbf{u}}_c R \, d\theta, \tag{5.3}$$

where the components of $\mathbf{u}$, $\mathbf{u}_c$ are given in $(3.6)_2$ and $(3.7)_2$.

6. Ring-to-shell joint

Due to the diversity of functions that the circular rings may play in the shell system (elements reinforcing the shell segments, boundary rings or elements joining two seg-

ments), it is convenient to write down the conditions of compatibility for the displacements of the rings and the shell in the global coordinate system x, θ, z. The geometrical relations between the displacements u_c, v_c, w_c, v_c of the cross-section centroids of the ring and the global components of displacement of the shell middle surface u^*, v^*, w^*, ϕ_1^* (Fig. 2) may be represented symbolically as $\bar{\mathbf{u}}_c = \mathbf{F}^*\mathbf{u}^*$, where

$$(6.1)\qquad \mathsf{F}_c^* = \left[\begin{array}{c|c|c|c} 1 & 0 & 0 & 0 \\ \hline -\frac{a_2}{r}\frac{d}{d\theta} & 1+\frac{a_1}{r} & -\frac{a_1}{r}\frac{d}{d\theta} & 0 \\ \hline 0 & 0 & 1 & -a_2 \\ \hline 0 & 0 & 0 & 1 \end{array}\right], \qquad \mathbf{u}^* = \begin{Bmatrix} u^* \\ v^* \\ w^* \\ \phi_1^* \end{Bmatrix}.$$

Next, employing the relations between the components of displacement in the global and the local system, that is $\mathbf{u}^* = \mathbf{G}^*\mathbf{u}$, the displacement of the cross-section centroids of the ring may be expressed through the three components of displacement of the shell middle surface

$$(6.2)\qquad \bar{\mathbf{u}}_c = \mathsf{F}_c\mathbf{u}, \qquad \mathsf{F}_c = \mathsf{F}_c^*\mathsf{G}^*.$$

7. The elastic and kinetic energy

The elastic and kinetic energy (3.2) of the shell segments and the circular rings may now be expressed only in terms of the displacements of the shell middle surface.

Substitution of the constitutive (5.1) and the kinematical (5.2) relations together with the relations (6.2) for the circular rings in the expressions for the elastic energy of the elements of the system yields

$$(7.1)\qquad E_s = \frac{1}{2}\int_s\int_\theta (\mathsf{A}_s\mathbf{u})^T\mathbf{C}_s\mathsf{A}_s\mathbf{u}\,r\,d\theta\,ds, \qquad E_c = \frac{1}{2}\int_\theta (\mathsf{A}_c\mathbf{u})^T\mathbf{C}_c\mathsf{A}_c\mathbf{u}R\,d\theta,$$

where

$$\mathsf{A}_c = \bar{\mathsf{A}}_c\mathsf{F}^*\mathsf{G}^*.$$

The same procedure may be applied to the kinetic energy. However, it is more convenient to write them in a modified form, separating the component parts of energy coming from the independent and dependent parameters of displacement. After appropriate decomposition of the vectors $\mathbf{u}_s$, $\mathbf{u}_c$ whose components are given in (3.5), and employing the relations (3.6), (3.7) and additionally (6.2), the kinetic energy may be written in the form

$$(7.2)\qquad T_s = \frac{\omega^2}{2}\int_s\int_\theta [\mathbf{u}^T\mathbf{M}_s\mathbf{u} + (\mathsf{B}_s\mathbf{u})^T\mathbf{J}_s\mathsf{B}_s\mathbf{u}]\,r\,d\theta\,ds,$$

$$T_c = \frac{\omega^2}{2}\int_s\int_\theta [(\mathsf{F}_c\mathbf{u})^T\mathbf{M}_c\mathsf{F}_c\mathbf{u} + (\mathsf{B}_c\mathsf{F}_c\mathbf{u})^T\mathbf{J}_c\mathsf{B}_c\mathsf{F}_c\mathbf{u}]\,R\,d\theta.$$

The entries in the matrices of inertia $\mathbf{M}_s$, $\mathbf{I}_s$, $\mathbf{M}_c$, $\mathbf{I}_c$ are as follows:

$$\mathbf{M}_s = \varrho_s h \mathbf{I}_{(3\times 3)}, \qquad \mathbf{J}_s = \varrho_s \frac{h^2}{12} \mathbf{I}_{(2\times 2)}$$

$$\mathbf{M}_c = \varrho_c A_c \operatorname{diag}\left[1, 1, 1, \frac{J_c}{A_c}\right], \qquad \mathbf{J}_c = \varrho_c \begin{bmatrix} J_{zc} - J_{xz} \\ -J_{xc} \quad J_{xc} \end{bmatrix},$$

where ϱ_c, ϱ_s are the densities of the shell and the ring, respectively, h is the thickness of the shell, A_c is the area of the cross-section of the ring and $\mathbf{I}_{zc}$, $\mathbf{I}_{xc}$, $\mathbf{I}_{xz}$, $\mathbf{I}_c$, are its moments of inertia. $\mathbf{I}$ stands for the unit matrices.

8. Solution of the problem

The functional H (see (3.1)), whose components are the elastic (7.1) and the kinetic (7.2) energies of the shell elements and the rings, has an integro-differential form. This functional will be now reduced to an algebraic quadratic form via separation of variables, expansion of the parameters of the displacement into trigonometric series in the circumferential direction and discretization in the meridional direction.

The displacement vector $\mathbf{u}$, which is a function of two variables s, θ, has been expanded in a trigonometric series in the circumferential direction in the following way:

$$\mathbf{u}(s, \theta) = \sum_{n=0}^{N} (\mathbf{T}_1^n \mathbf{u}_1^n + \mathbf{T}_2^n \mathbf{u}_2^n), \tag{8.1}$$

where $\mathbf{T}_1^n$, $\mathbf{T}_2^n$ are diagonal trigonometric matrices

$$\mathbf{T}_1^n = \operatorname{diag}[\sin n\theta, \cos n\theta, \sin n\theta], \quad \mathbf{T}_2^n = \operatorname{diag}[\cos n\theta, \sin n\theta, \cos n\theta].$$

Vectors $\mathbf{u}_1^n$ are skew-symmetric and $\mathbf{u}_2^n$—symmetric components of the displacement vector $\mathbf{u}$. Such expansion of $\mathbf{u}$ enables us to carry out exact integration of the expressions for energy with respect to the circumferential variable θ. For instance, integrating the elastic energy of the shell segment $(7.1)_1$ one can obtain

$$\sum_{\alpha,\beta=1}^{2} (\mathsf{A}_s \mathbf{T}_\alpha^k \mathbf{u}_\alpha^k)^T \mathbf{C}_s \mathsf{A}_s \mathbf{T}_\beta^n \mathbf{u}_\beta^n r \, d\theta = (\mathsf{A}_{s\alpha}^k \mathbf{u}_\alpha^k)^T \mathbf{C}_{s\alpha\beta}^{kn} \mathsf{A}_{s\beta}^n \mathbf{u}_\beta^n, \qquad k, n = 0, 1, \ldots, N.$$

The operators $\mathsf{A}_{s\alpha}^n$ resulted from differentiation of the operators A_s with respect to θ, and the matrices $\mathbf{C}_{s\alpha\beta}^{kn}$ have the form

$$\mathbf{C}_{s\alpha\beta}^{kn} = \delta_{\alpha\beta} \delta_{kn} r \mathbf{C}_s \operatorname{diag}[(1 \pm \delta_{n0}), (1 \pm \delta_{n0}), (1 \mp \delta_{n0}), (1 \pm \delta_{n0}), (1 \pm \delta_{n0}), (1 \mp \delta_{n0}], \tag{8.2}$$

where $\delta_{\alpha\beta}$, δ_{kn} are Kronecker deltas. In the diagonal matrices above, the upper signs refer to the case $\alpha = \beta = 1$, and the lower ones to the case $\alpha = \beta = 2$.

The operator $\mathsf{A}_{c\alpha}^n$ and the matrix $\mathbf{C}_{c\alpha\beta}^{kn}$ connected with the circular ring, can be obtained in an identical way. We can write this matrix as follows:

$$\mathbf{C}_{c\alpha\beta}^{kn} = \delta_{\alpha\beta} \delta_{kn} R C_c \operatorname{diag}[(1 \mp \delta_{n0})(1 \mp \delta_{n0}), (1 \mp \delta_{n0}), (1 \pm \delta_{n0})]. \tag{8.3}$$

Absence of couplings between the components of the trigonometric series (8.1), stemming from the form of the matrices $\mathbf{C}^{kn}_{s\alpha\beta}$ (8.2) and $\mathbf{C}^{kn}_{c\alpha\beta}$ (8.3), allows to write the components of the elastic energy for a single reinforced shell segment in the following form:

$$E_s = \frac{\pi}{2}(1+\delta_{n0}) \sum_{n=-N}^{N} \int_s (\mathbf{A}^n_s \mathbf{u}^n)^T \mathbf{C}^n_s \mathbf{A}^n_s \mathbf{u}^n ds,$$

(8.4)

$$E_c = \frac{\pi}{2}(1+\delta_{n0}) \sum_{n=-N}^{N} \sum_{c=1}^{C} (\mathbf{A}^n_c \mathbf{u}^n)^T \mathbf{C}^n_c \mathbf{A}^n_c \mathbf{u}^n,$$

where $\mathbf{C}$ is the number of rings on this segment.

We have introduced the following conventions in Eq. (8.4) for the sake of brevity:

$$\mathbf{u}^n = \begin{cases} \mathbf{u}^k_1 & \text{for} \quad n > 0, \\ \mathbf{u}^k_2 & \text{for} \quad n < 0, \\ \mathbf{T}^0_1 \mathbf{u}^0_1 + \mathbf{T}^0_2 \mathbf{u}^0_2 & \text{for} \quad k = 0, \end{cases} \qquad k = 1, 2, \ldots, N,$$

$$\mathbf{A}^n_q = \begin{cases} \mathbf{A}^k_{q1} & \text{for} \quad n > 0, \\ \mathbf{A}^k_{q2} & \text{for} \quad n < 0, \\ \mathbf{A}^0_{q1} = \mathbf{A}^0_{q2} & \text{for} \quad n = 0, \end{cases} \qquad k = 1, 2, \ldots, N, \quad q = s, c, \tag{8.5}$$

$$\mathbf{C}^n_q = \begin{cases} \mathbf{C}^{kk}_{q11} = \mathbf{C}^{kk}_{q22} & \text{for} \quad n > 0 \quad \text{and} \quad n < 0, \\ \mathbf{C}^{00}_{q11} = \mathbf{C}^{00}_{q22} & \text{for} \quad n = 0, \end{cases} \qquad k = 1, 2, \ldots, N, \quad q = s, c.$$

Having applied the same procedures to the terms of kinetic energy (7.2) and after integration with respect to θ, we obtain

$$T_s = \omega^2 \frac{\pi}{2}(1+\delta_{n0}) \sum_{n=-N}^{N} \int_s [(\mathbf{u}^n)^T \mathbf{M}^n_s \mathbf{u}^n + (\mathbf{B}^n_s \mathbf{u}^n)^T \mathbf{J}^n_s \mathbf{B}^n_s \mathbf{u}^n] ds,$$

(8.6)

$$T_c = \omega^2 \frac{\pi}{2}(1+\delta_{n0}) \sum_{n=-N}^{N} \sum_{c=1}^{C} [(\mathbf{F}^n_c \mathbf{u}^n)^T \mathbf{M}^n_c \mathbf{F}^n_c \mathbf{u}^n + (\mathbf{B}^n_c \mathbf{F}^n_c \mathbf{u}^n)^T \mathbf{J}^n_c \mathbf{B}^n_c \mathbf{F}^n_c \mathbf{u}^n].$$

The notation in (8.6) is identical with that used in (8.5), and the matrices of inertia have the form:

$$\begin{aligned} \mathbf{M}^{kn}_{s\alpha\beta} &= \delta_{\alpha\beta}\delta_{kn} r \mathbf{M}_s \operatorname{diag}(1 \mp \delta_{n0}), (1 \pm \delta_{n0}), (1 \mp \delta_{n0}), \\ \mathbf{J}^{kn}_{s\alpha\beta} &= \delta_{\alpha\beta}\delta_{kn} r \mathbf{J}_s \operatorname{diag}(1 \mp \delta_{n0}), (1 \pm \delta_{n0}), \\ \mathbf{M}^{kn}_{c\alpha\beta} &= \delta_{\alpha\beta}\delta_{kn} R \mathbf{M}_c \operatorname{diag}(1 \mp \delta_{n0}), (1 \pm \delta_{n0}), (1 \mp \delta_{n0}), (1 \mp \delta_{n0}), \\ \mathbf{J}^{kn}_{c\alpha\beta} &= \delta_{\alpha\beta}\delta_{kn} R \mathbf{J}_c (1 \pm \delta_{n0}). \end{aligned} \tag{8.7}$$

The sign convention for the entries in the diagonal matrices remains the same, too.

Within each segment the meridian of the shell has been divided in to m subsegments. In each of these subsegments the geometrical parameters of the shell have been replaced with discrete values. The derivatives with respect to the meridional variable s have been replaced with central finite differences [2]. The displacements of the shell middle surface has been expressed through the displacements of discrete points on the shell meridian.

The integral within respect to the meridional variable s has been replaced by a sum of integrals calculated on each subsegment Δ_i. The fictitious points, lying beyond the boundaries of the shell and introduced to unify the notation, are eliminated via the relations linking these points with the true boundary displacements ϕ_A, u_A, v_A, w_A and ϕ_B, u_B, v_B, w_B for $s = s_A$ and $s = s_B$, respectively. Eventually, the integro-differential functional H can be transformed to the following algebraic form

$$\bar{H} = \sum_{n=-N}^{N} \sum_{p=1}^{P} \sum_{i=1}^{m_p} (\mathbf{u}_i^{pn})^T (\mathbf{K}_{pi}^n - \omega^2 \mathbf{M}_{pi}^n) \mathbf{u}_i^{pn}, \tag{8.8}$$

where

$$\begin{aligned} \mathbf{K}_{pi}^n &= (\mathbf{A}_{si}^{pn})^T \mathbf{C}_{si}^{pn} \mathbf{A}_{si}^{pn} \Delta_i + \delta_{ij} \sum_{c=1}^{C} \delta_{cj} (\mathbf{A}_{cj}^{pn})^T \mathbf{C}_{cj}^{pn} \mathbf{A}_{cj}^{pn}, \\ \mathbf{M}_{pi}^n &= \mathbf{M}_{si}^{pn} + (\mathbf{B}_{si}^{pn})^T \mathbf{J}_{si}^{pn} \mathbf{B}_{si}^{pn} + \delta_{ij} \sum_{c=1}^{C} \delta_{cj} \{(\mathbf{F}_{cj}^{pn})^T [\mathbf{M}_{cj}^{pn} + (\mathbf{B}_{cj}^{pn})^T \mathbf{J}_{cj}^{pn} \mathbf{B}_{cj}^{pn}] \mathbf{F}_{cj}^{pn}\}. \end{aligned} \tag{8.9}$$

m_p determines the number of subsegments in the segment p, and P — the number of the shell segments. Local stiffness matrices $\mathbf{K}_{pi}^n$ and matrices of inertia $\mathbf{M}_{pi}^n$ in the segment p are calculated as a sum of the respective local matrices for the shell and the ring, as shown in (8.9). The Kronecker delta δ_{ij}, appearing there, determines the location of the joint between the ring and the segment. The matrices $\mathbf{A}_{sj}^{pn}$, $\mathbf{A}_{cj}^{pn}$, $\mathbf{B}_{si}^{pn}$, $\mathbf{B}_{ci}^{pn}$ and $\mathbf{F}_{cj}^{pn}$ resulting from the relevant operations A_s^n, A_c^n, B_s^n, B_c^n and F_c^n after application of the finite differences, whereas the matrices of stiffness $\mathbf{C}_{si}^{pn}$, $\mathbf{C}_{cj}^{np}$ and inertia $\mathbf{M}_{si}^{pn}$, $\mathbf{J}_{si}^{np}$, $\mathbf{M}_{cj}^{pn}$, $\mathbf{J}_{cj}^{pn}$ are the matrices described by (8.2), (8.3) and (8.7), calculated for each respective subsegment. Summation with respect to the indices i and p, appearing in (8.8), is carried out by introduction of the global vectors $\tilde{\mathbf{u}}^n$ and matrices $\mathbf{K}^n$ and $\mathbf{M}^n$, reduced suitably to the boundary constraints imposed.

The functional $\bar{H}$ (8.8) may also be represented in the form (8.10)

$$\bar{H} = \sum_{n=-1}^{N} (\tilde{\mathbf{u}}^n)^T (\mathbf{K}^n - \omega^2 \mathbf{M}^n) \tilde{\mathbf{u}}^n. \tag{8.10}$$

The stationarity condition for the quadratic form (8.10), due to the absence of couplings between the harmonics and the relation stemming from the existence of symmetry with respect to the xz plane

$$\begin{aligned} (\tilde{\mathbf{u}}^n)^T \mathbf{K}^n \tilde{\mathbf{u}}^n &= (\tilde{\mathbf{u}}^k)^T \mathbf{K}^k \tilde{\mathbf{u}}^k, \quad n = 1, 2, \ldots, N, \\ (\tilde{\mathbf{u}}^n)^T \mathbf{M}^n \tilde{\mathbf{u}}^n &= (\tilde{\mathbf{u}}^k)^T \mathbf{M}^k \tilde{\mathbf{u}}^k, \quad k = -1, -2, \ldots, -N, \end{aligned}$$

leads to $N+1$ eigen-value problems

$$\mathbf{K}^n \tilde{\mathbf{u}}^n = \omega^2 \mathbf{M}^n \tilde{\mathbf{u}}^n, \quad n = 0, 1, \ldots, N. \tag{8.11}$$

The matrices $\mathbf{K}^n$ and $\mathbf{M}^n$ are symmetric banded matrices. Moreover, the matrices of inertia $\mathbf{M}^n$ are positive definite. The definiteness of the stiffness matrix $\mathbf{K}^n$ depends on the boundary conditions imposed.

The solution to the $N+1$ generalized eigen-value problems (8.11) gives the free vibration frequencies and the corresponding modes for the segmented shell of revolution reinforced with circular rings.

11. Numerical calculations

Basing on the algorithm presented above, a program DYSAR written in Fortran IV has been implemented on the R-32 computer in the Institute of Fluid Flow Machinery of Polish Academy of Sciences in Gdańsk. This program has been tested in a number of examples. One of them which we are going to present below was the test of convergence of the finite difference method.

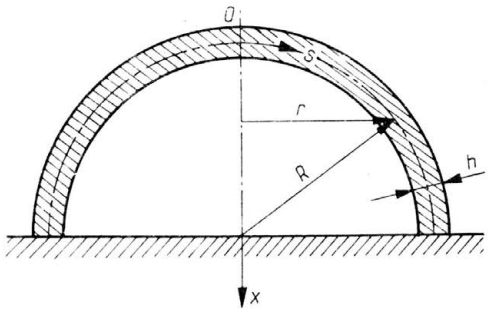

FIG. 3. Geometry and material constants of the spherical shell. $R = 2.54$ m, $h = 0.0254$ m, $E = 2.48 \cdot 10^5 \mathrm{Nm}^{-2}$, $\nu = 0.3$, $\varrho = 10.69\ \mathrm{Ns}^2\mathrm{m}^{-4}$.

The object considered was a hemisphere (Fig. 3). The results obtained were compared with those published by BUSHNELL [5] and ZARGHAMEE and ROBINSON [20]. Let us mention here that Bushnell applied NOVOZHILOV'S variant of the linear shell theory [13], whereas the paper [20] is based on FLÜGGE'S equations [8]. One should expect, though, that in this case the influence of the variant of the theory chosen is negligible. The material constants of the shell (Fig. 3) were taken from BUSHNELL [5].

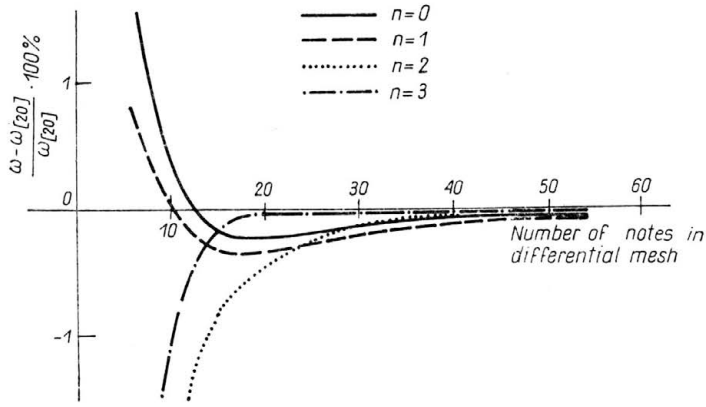

FIG. 4. Convergence of the lowest frequencies for $n = 0, 1, 2, 3$ in comparison to [20] versus the number of division of the shell meridian.

A few lowest frequencies, corresponding to the circumferential wave numbers $n = 0$, 1, 2, 3, where calculated for different divisions of the shell meridian. Figure 4 illustrates the convergence of the frequencies for each circumferential wave number n versus the division of the meridian in comparison with the solution from [20]. The graph shows that already at the division into 12 subsegments (13 knots of the finite difference mesh) the difference with respect to [20] does not exceed 2%, and at 20 knots mesh, for all circumferential wave numbers n, this difference amounts only to $\sim 0.3\%$.

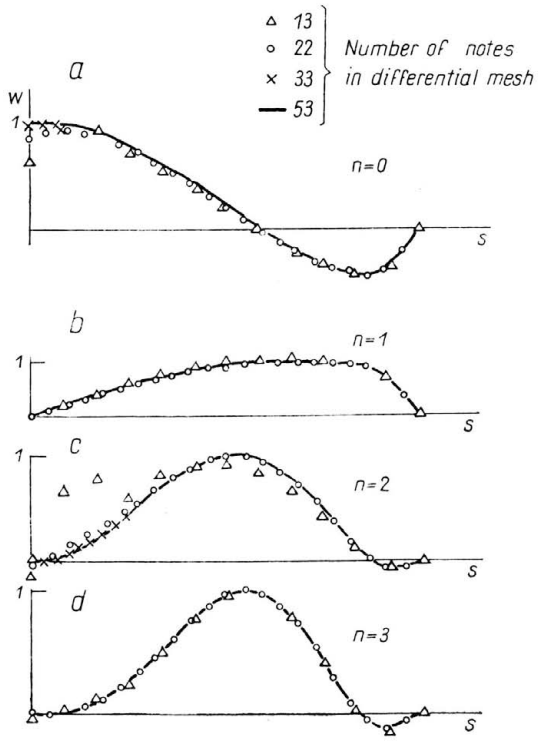

FIG. 5. Convergence of the bending modes of free-vibrations corresponding to the lowest frequencies for $n = 0, 1, 2, 3$ versus the number of division of the shell meridian.

The convergence of the corresponding modes is shown in the Fig. 5. The modes are normalized with respect to the matrices of stiffness and inertia, that is $(\tilde{\mathbf{u}}^n)^T\mathbf{K}^n\tilde{\mathbf{u}}^n = \omega_k^2$, $(\tilde{\mathbf{u}}^n)^T\mathbf{M}^n\tilde{\mathbf{u}}^n = 1$. A distinct correlation between the convergence of the frequencies and modes is noticable (compare Figs. 4 and 5). The local perturbations of mode shapes in the neighbourhood of the shell apex result from geometrical singularity at this point (e.g. Fig. 5a, c). In this particular problem the total error comprises the error stemming from too thin finite difference mesh and the error coming from the singularity in the point $x = 0$ (Fig. 3). Due to the singularity in this point ($r = 0$), the energy of the shell was not calculated in the point $x = 0$, but at a distance from it, equal to $\Delta/4$ (here Δ is the length of the subsegment in the finite difference scheme).

The rest of convergence discussed above seems to give satisfying results.

The Fig. 6 shows schematically the modes obtained for $n = 0, 1, 2, 3$.

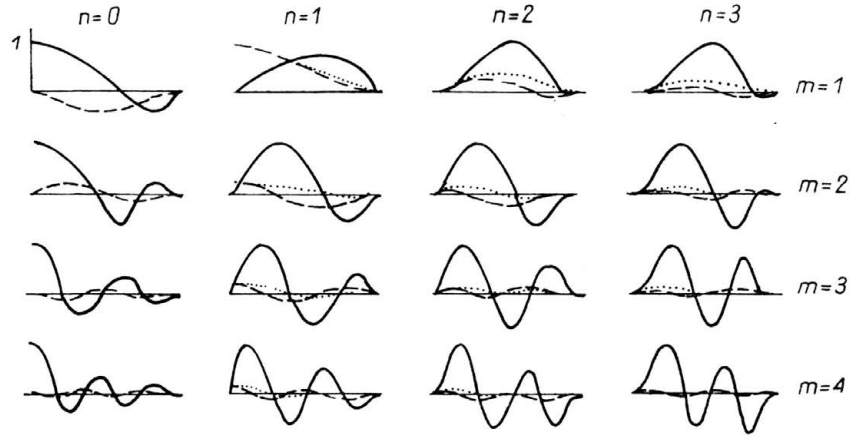

FIG. 6. Free vibration modes of the hemisphere.

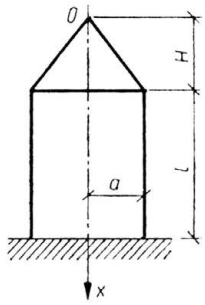

FIG. 7. Geometry and physical data of the segmented shell (cone-cylinder): $a = 0.1270$ m, $l = 0.3048$ m, $H = 0.1524$ m, $E = 6.89 \cdot 10^{10}$N m^{-2}, $\nu = 0.3$, $\varrho = 2.767 \cdot 10^3$ N s^2 m^{-4}, $h = 0.81 \cdot 10^{-3}$ m. Boundary conditions: for $x = 0$—$N_{11} = T = Q = M_{11} = 0$, for $x = l+H$—$\phi_1 = u = v = w = 0$.

The second example is a two-segment shell. One of the segments is conical and the other cylindrical (Fig. 7). The cone was divided into 10 subsegments and the cylinder into 15. The relation between the frequencies and the circumferential wave number is shown in the Fig. 8. This figure also shows experimental results obtained by Lashkari and Weingarten [12]. These experimental results lead to the conclusion that some of the frequencies correspond to such modes that each of the two segments vibrates with different circumferential wave number n. The graph of frequencies contains two minima (Fig. 8). This indicates the existence of frequencies near or equal to each other and the possibility of vibrations with complex modes. For instance, the composition of the mode $n = 4$, $m = 2$, $\omega = 1099$ Hz and the mode $n = 7$, $m = 2$, $\omega = 1097$ Hz results in a mode, for which each of two segments vibrates with a different circumferential wave number (the cone with $n = 4$ and the cylinder with $n = 7$) (Fig. 9). The following normalization has been assumed for the graph in the Fig. 9: $(\tilde{\mathbf{u}}^n)^T\mathbf{K}^n\tilde{\mathbf{u}}^n = \omega^2$, $(\tilde{\mathbf{u}}^n)^T\mathbf{M}^n\tilde{\mathbf{u}}^n = 1$. Of course, vibrations composed of more than two modes are also possible, for example of the modes:

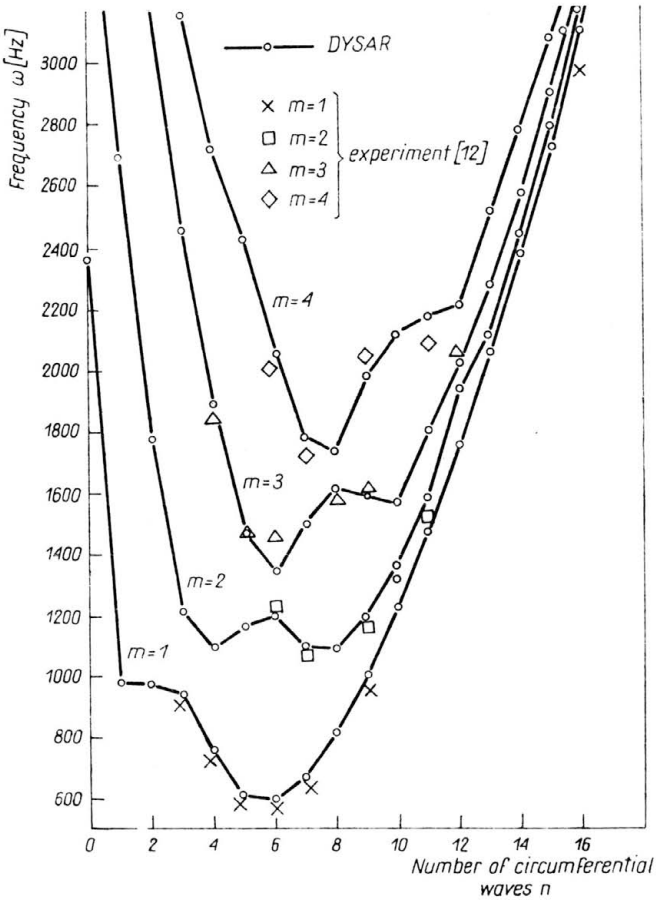

FIG. 8. Free vibration frequencies ω[Hz] of the shell cone-cylinder versus the number n of circumferential waves.

$n = 4, m = 2, \omega = 1099$ Hz; $n = 7, m = 2, \omega = 1097$ Hz and $n = 8, m = 2, \omega = 1100$ Hz. Experimental "grasping" of such complex vibrations may turn out to be difficult. Due to the singularity at the top of the case the energies were calculated at a distance $\Delta/4$ from the top, where Δ is the length of the subsegment in finite difference mesh.

The last example is a simply supported conical shell reinforced with three circumferential rings (Fig. 10).

The meridian of the shell was divided into 18 subsegments. Figure 11 shows how ω depends on n according to the results obtained with the aid of the program DYSAR. It also shows the comparison with the results obtained in [7]. The dependence of ω on n for a shell without rings is shown in the Fig. 12. The comparison of the two cases, that is of the shells with and without rings, leads to the conclusion that the stiffeners may change the mode corresponding to the lowest frequency, for in this example the lowest frequency of the shell with rings is $\omega = 1228{,}1$ Hz and corresponds to the mode $m = 1$,

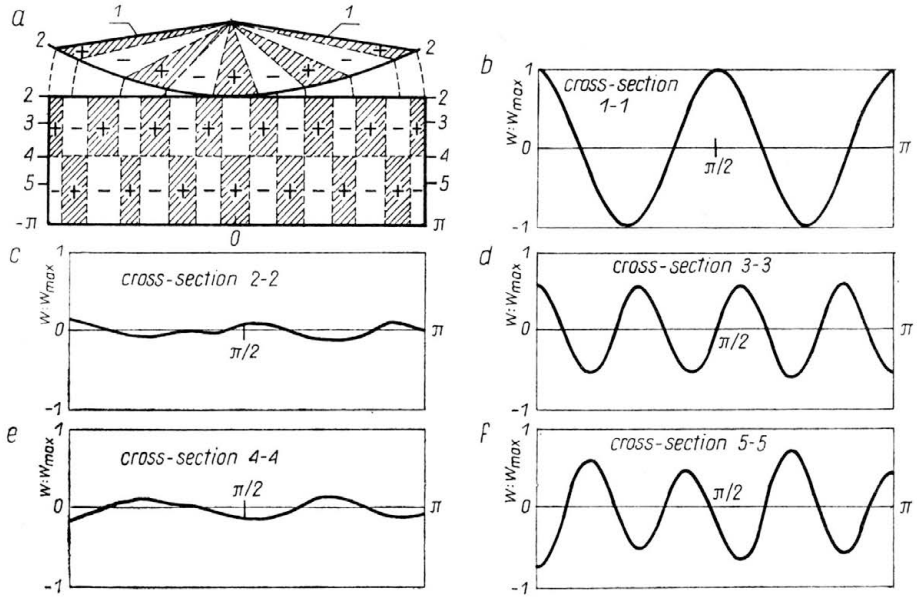

FIG. 9. Composition of the modes: $n = 4$, $m = 2$ ($\omega = 1099$ Hz); and $n = 7$, $m = 2$ ($\omega = 1097$ Hz), a) development of the shell cone-cylinder, b) –f) the modes in the subsequent cross-sections.

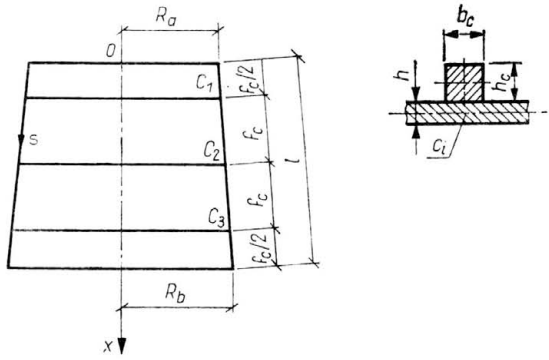

FIG. 10. Geometry and material data of the conical shell and the rings. Shell: $R_a = 8.6995\ 10^{-2}$ m, $R_b = 0.1334$ m, $l = 0.2667$ m, $h = 2.54 \cdot 10^{-3}$m, $E = 6.83 \cdot 10^{10}$Nm^{-2}, $\nu = 0.303$, $\varrho = 2.71 \cdot 10^3$ Ns^2 m^{-4}. Ring: $b_c = 6.35 \cdot 10^{-3}$ m, $h_c = 6.35 \cdot 10^{-3}$ m, $f_c = 8.89 \cdot 10^{-2}$ m $E_c = 6.83 \cdot 10^{10}$ Nm^{-2}, $\nu_c = 0.303$, $\varrho_c = 2.71 \cdot 10^3$ Ns^{2}m^{-4}. Number of rings: 3, C_i ($i = 1, 2, 3$) — ring attachment points to the shell. Boundary conditions: for $s = 0$, l—$N_{11} = v = w = M_{11} = 0$.

$n = 3$, whereas for the shell without rings the respective frequency is $\omega = 1060{,}4$ Hz and corresponds to the mode $m = 1$, $n = 1$. Additional stiffeners, in the case, increase the basic free vibration frequencies by 15,8% as compared to the non-stiffened shell. Figure 13 shows typical modes obtained for the conical shell under discussion. The modes of the type a) and c) were obtained for the harmonics $n = 1 \div 4$. Starting with $n = 5$ the bending vibrations vanish in the upper portion of the cone. The phenomenon of shortening of wavelength with the increase in the circumferential wavelength number n occurs. This phenomenon was described by WEINGARTEN [18]. However, with the increase in the num-

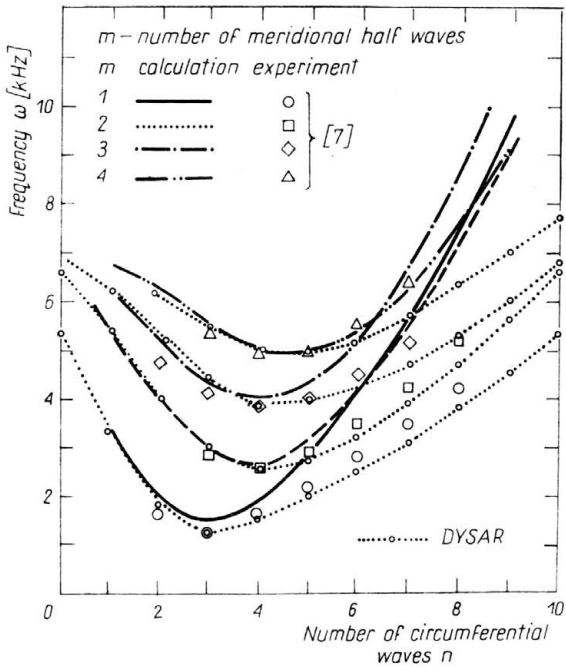

FIG. 11. ω versus n for the conical shell with 3 rings.

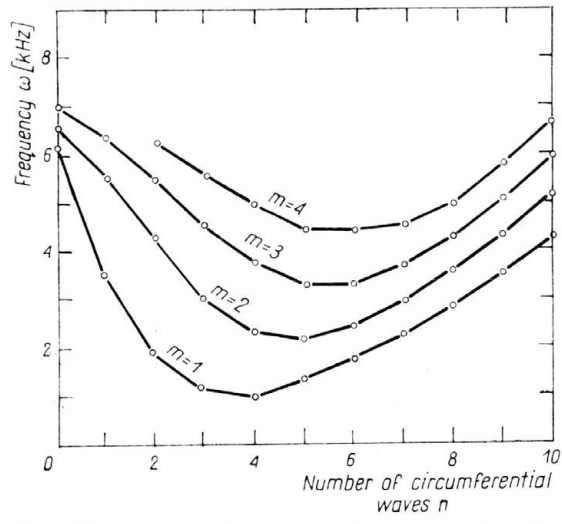

FIG. 12. ω versus n for a non-stiffened conical shell.

ber m of half-waves along the meridian of the shell, significant differences between the modes of vibration for a stiffened and non-stiffened shell can be observed (e.g. $n = 8$, $m = 4$, fig. 13). It was also observed that attachment of rings results in occurence of additional local bends in the shapes of modes in the neighbourhood of the points of attachment (Fig. 13).

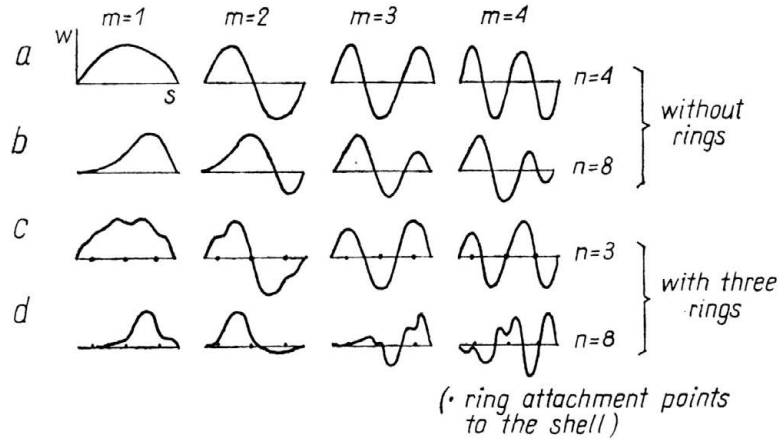

FIG. 13. Typical bending free vibration modes for a simply supported conical shell.

12. Final remarks and conclusions

The analysis of the model and the numerical examples show that the rings do not cause couplings between the circumferential wave numbers n. So, formally, the analysis of free vibration of segmented shells of revolution with rings may be decoupled and thus converted into $N+1$ separate eigen-value problems, as it happens to be with the smooth shells. However, due to the concentration of frequencies in the spectrum, the real free vibration modes may be linear combinations of the classical modes connected with the same or proximate frequencies (Fig. 9). Besides, rings as well as angular joints between the segments may confine the vibrations of the shell only to some of its regions.

Numerical tests proved the effectiveness of the method presented here. Comparison of the results obtained with the aid of the program DYSAR with the experimental data from the literature indicates accuracy sufficient for practical purposes even at the relatively small number of finite difference mesh.

It is noteworthy that the method presented and the program DYSAR may be used in the free vibration analysis of stiffened or non-stiffened fragments of shells of revolution and (with adequately elected geometrical parameters) of rectangular plates (fragment of a cylinder of a very large radius), provided the boundary conditions comply with the requirements of rotational symmetry.

References

1. M. S. ANDERSON, R. E. FULTON, W. L. HEARD, J. E. WALZ, *Stress, buckling and vibration analysis of shells of revolution*, Computers and Structures, 1, 157–192, 1971.
2. B. BŁOCKA, *Free vibrations of segmented, stiffened shells of revolution* [in Polish], PhD Thesis, Institute of Fluid Flow Machinery, nr 69/85, Gdańsk 1985.
3. B. BŁOCKA, *Free vibrations of thin, elastic, orthogonally stiffened shells of revolution with stiffeners treated as discrete elements* [to appear in Enging. Trans., 1989].

4. D. BUSHNELL, *Analysis of buckling and vibration of ring-stiffened segmented shells of revolution*, Intern. J. Solids Struct., 6, 157–181, 1970.
5. D. BUSHNELL, *Finite-difference energy models versus finite-element models: two variational approaches in one computer program*, in: Numerical and Computer Methods in Structural Mechanics, ed. by S. J. FENVES *et al.*, Academic Press, 1973.
6. G. A. COHEN, *Computer analysis of symmetric free vibrations of ring-stiffened orthotropic shells of revolution*, AIAA J., 3, 12, 2305–2312, 1965.
7. D. E. CRENWELGE Jr., D. MUSTER, *Free vibrations of ring- and stringer-stiffened conical shells*, The Journal of the Acoustical Society of America, 46, 1, 176–185, 1969.
8. W. FLÜGGE, *Stresses in shells*, Springer Verlag, Berlin 1966.
9. J. GOŁAŚ, Z. KASPERSKI, *Numerical calculations of shells of revolution by finite element method* [in Polish], PWN, Warszawa 1978.
10. В. С. Гонткевич, *Собственные колебания пластинок и оболочек*, Наукова Думка, Киев 1964.
11. A. KALNINS, *Free vibration of rotationally symmetric shells*, The Journal of the Acoustical Society of America, 36, 7, 1355–1365, 1964.
12. M. LASHKARI, V. I. WEINGARTEN, *Vibration of segmented shells*, Experimental Mech., 13, 120–125, 1973.
13. V. V. NOVOZHILOV, *The theory of thin shell*, Wolters Nordhooff, Groningen 1970.
14. G. RAKOWSKI, R. SOLECKI, *Curved rods. Statical calculations* [in Polish], ARKADY, Warszawa 1966.
15. J. L. SANDERS Jr., *An improved first approximation theory for thin shells*, NASA TR-R24, 1959.
16. S. K. SEN, P. L. GOULD, *Free vibrations of shells of revolution using FEM*, J. Enging. Mech. Division EM2, 283–303, 1974.
17. V. SVALBONAS, J. KEY, *Static, stability, and dynamic analysis of shells of revolution by numerical integration— a comparison*, Nuclerar Enging. and Design, 27, 30–45, 1974.
18. V. I. WEINGARTEN, *Free vibration of ring-stiffened conical shells*, AIAA J. 8, 1475–1481, 1965.
19. J. WILSON, *Vibration of axisymmeric shells*, in: Vibration of Engineering Structures, ed. by C. E. BREBBIA, *et al.*, 255–280, Soupthamton 1975.
20. M. S. ZARGHAMEE, A. R. ROBINSON, *A numerical method for analysis of free vibration of spherical shells*, AIAA J., 5, 7, 1256–1261, 1967.

POLISH ACADEMY OF SCIENCES
INSTITUTE OF FLUID FLOW MACHINERY, GDAŃSK.

Received December 19, 1986.